The Jahn−Teller Effect in CH_3CN^+ ($\tilde{X}^2E$) and CD_3CN^+ ($\tilde{X}^2E$) Studied by Zero Kinetic Energy Photoelectron Spectroscopy

Jie Yang, Chang Zhou, and Yuxiang Mo*

Department of Physics and Key Laboratory for Atomic and Molecular Nanosciences, Tsinghua University, Beijing, 100084 China

Received: August 5, 2005; In Final Form: September 2, 2005

The Jahn−Teller effect in CH_3CN^+ ($\tilde{X}^2E$) and CD_3CN^+ ($\tilde{X}^2E$) has been found experimentally by zero kinetic energy (ZEKE) photoelectron spectroscopy using coherent extreme ultraviolet (XUV) radiation. The vibronic bands of CH_3CN^+ ($\tilde{X}^2E$) and CD_3CN^+ ($\tilde{X}^2E$) at about 4500 cm^{-1} above the ground states have been recorded. The spectra consist mainly of the Jahn−Teller active C−C≡N bending (υ_8), the C≡N stretching (υ_2), the CH_3 (CD_3) deforming (υ_6), and the C−C stretching (υ_4) vibronic excitations. The Jahn−Teller active vibronic bands (υ_8) have been assigned with a harmonic model including linear and quadratic Jahn−Teller coupling terms, taking into account only the single mode vibronic excitation. The ionization potentials of CH_3CN and CD_3CN have also been determined, and their values are 12.2040(±0.001) and 12.2286(±0.001) eV, respectively.

I. Introduction

The vibrational structures of the acetonitrile cation and its deuterium cation (CH_3CN^+ and CD_3CN^+) have been studied by photoionization mass spectrometry (PI)[1−4] and photoelectron spectroscopy (PE).[5−8] The most recent PE study with the highest resolution was published more than 10 years ago and had an instrumental resolution of 25 meV (∼200 cm^{-1}), which is apparently low for obtaining vibrationally resolved structure information.[8] Therefore, only very limited information about the vibrational structures of CH_3CN^+ and CD_3CN^+ are known at present. The neutral CH_3CN and CD_3CN have the C_{3v} geometrical structures and the outmost valence molecular orbitals for them can be represented as $(4a_1)^2(5a_1)^2(6a_1)^2(1e)^4(7a_1)^2(2e)^4$:$^1A'$.[9,10] If the geometric structures of CH_3CN^+ ($\tilde{X}$) and CD_3CN^+ ($\tilde{X}$) also have the C_{3v} symmetries, the expected electronic configurations for them should be $\cdots(2e)^3$:^2E. As is well-known, the energy levels for the degenerate vibrational modes will be split due to the coupling of the electronic motion with the vibrational motion (vibronic coupling). This is the so-called Jahn−Teller effect (see refs 11−13 for recent reviews).

From the observation of the single quantum excitation of the degenerate C−C≡N bending vibration (υ_8) in the photoionization efficiency curves[4] and also in the He(I) photoelectron spectra,[8] Jahn−Teller coupling was proposed to be present in them. This is because the single quantum excitation of the degenerate vibrational band is usually not observable if the Jahn−Teller effect is not present. However, the energy-level splittings arising from the Jahn−Teller effect in CH_3CN^+($\tilde{X}$) and CD_3CN^+($\tilde{X}$) have not been observed until now.

The geometries of CH_3CN^+ ($\tilde{X}$)and CD_3CN^+ ($\tilde{X}$) have not been determined experimentally. A recent calculation employing the DFT method showed that the geometric structure of CH_3CN^+ ($\tilde{X}$) has the C_s symmetry, and hence, the bending vibration becomes nondegenerate.[14] If this is true, the single quantum excitation of the C−C≡N bending excitation should be observable without taking the Jahn−Teller effect into consideration. Therefore, vibrationally resolved structure studies for CH_3CN^+ ($\tilde{X}$)and CD_3CN^+ ($\tilde{X}$) are needed to provide concrete evidence of the Jahn−Teller coupling in them. The Jahn−Teller effect in CX_3Y type molecules, such as CH_3O, has been extensively studied.[11,15,16] The multimode interaction in CX_3Y makes them difficult to analyze theoretically. However, for CH_3CN^+ and CD_3CN^+, because of the low values of the C−C≡N bending fundamental frequencies (∼300 cm^{-1}), the multimode interaction for the first several vibronic bands is expected to be weak. Thus, CH_3CN^+ and CD_3CN^+ may provide a very interesting example of a single mode Jahn−Teller effect.

In another respect, the accurate ionization potentials (IP) of CH_3CN and CD_3CN are important for their thermochemistry. The present most accurate IP of CH_3CN and CD_3CN have uncertainties around 5 meV (40 cm^{-1}) and were obtained by PE and PI methods.[17] There are very few measurements of IP for CD_3CN.[17]

In this paper, we report a study of the vibronic structures for CH_3CN^+ ($\tilde{X}^2E$) and CD_3CN^+ ($\tilde{X}^2E$), employing the pulse field ionization and zero kinetic energy photoelectron (PFI-ZEKE) spectroscopy[18,19] and the coherent extreme ultraviolet (XUV) radiation. Their vibrational structures show clearly the vibronic coupling or the Jahn−Teller effect in them. The ionization potentials of CH_3CN and CD_3CN have also been determined accurately.

II. Experimental Section

The XUV photoelectron and photoion spectrometer used in this work has been described recently.[20,21] Coherent XUV radiation was generated by using the resonance enhanced four-wave sum mixing in a pulsed Xe jet. A Nd:YAG (20 Hz) pumped two dye laser system was used to prepare the fundamental frequency laser beams. One beam produced by doubling the dye laser frequency was fixed to match the two-photon resonance ($2\omega_1$) frequency of the Xe $5p^5(^2P_{3/2})6p[1/2]_0 \leftarrow (5p^6)^1S_0$ transition at 80 119.0 cm^{-1}. The other beam (ω_2)

* To whom correspondence should be addressed. E-mail: ymo@mail.tsinghua.edu.cn.

10.1021/jp054366f CCC: $30.25
Published on Web 10/13/2005

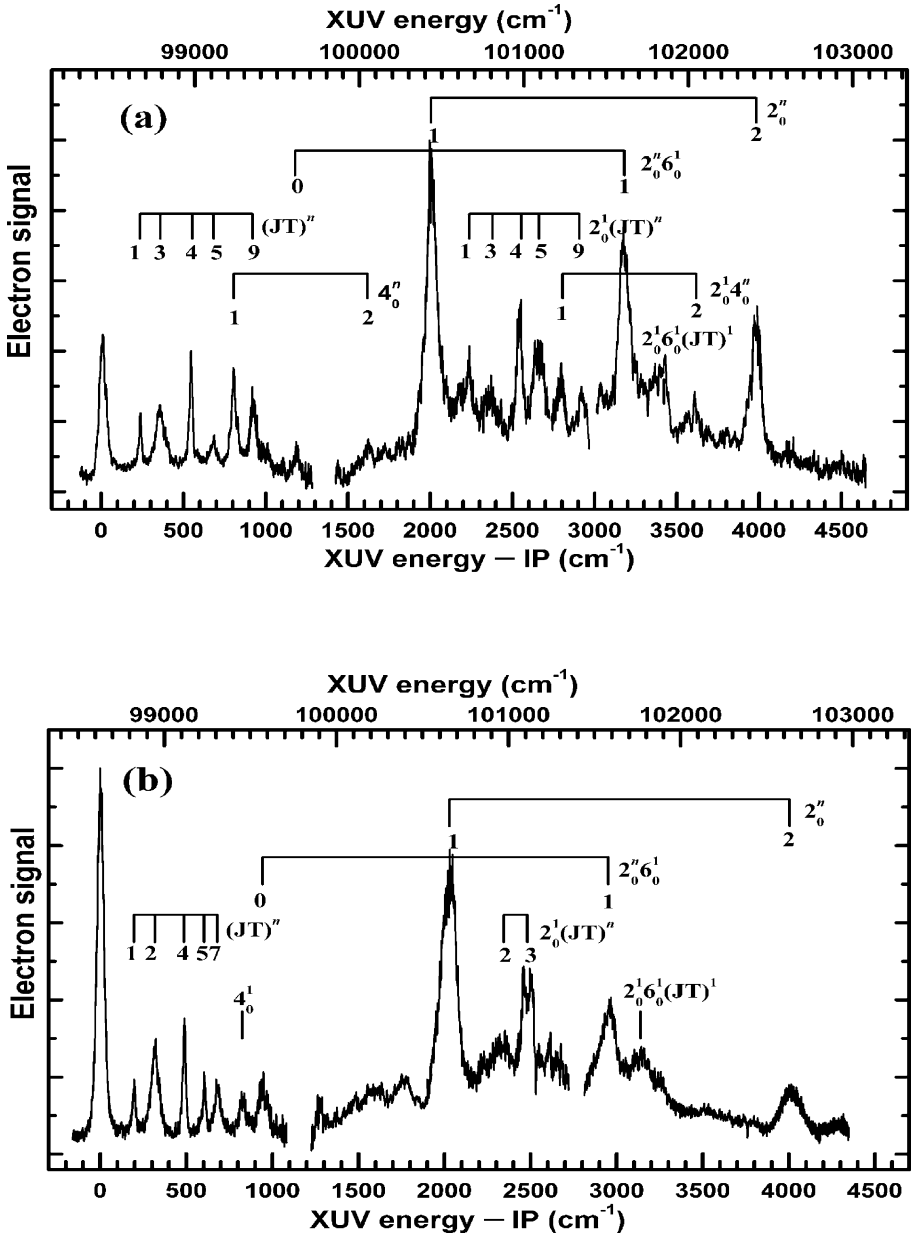

Figure 1. PFI-ZEKE spectra of (a) CH_3CN and (b) CD_3CN. The pulse electric field strengths used to ionize the Rydberg molecules were 0.85 V/cm. On the *x*-axis at the top are the XUV photon energies, and on the *x*-axis at the bottom are XUV photon energies relative to the ionization potentials of CH_3CN and CD_3CN. The vibrational bands 2_0^n, 4_0^n, and 6_0^n represent the C≡N stretching (υ_2), the C−C stretching (υ_4), and the CH_3 (CD_3) deforming (υ_6) vibronic excitations from the ground state to the *n*th vibronic states, respectively. $(JT)^n$ represents the Jahn−Teller active C−C≡N bending (υ_8) vibronic excitation.

was tuned from 435 to 550 nm by using different laser dyes. The two fundamental beams were merged by a dichroic mirror and focused by an achromatic lens (250 mm) into a pulsed Xe jet. The apparatus consists of four vacuum chambers, namely: (a) the frequency mixing chamber, which houses the pulse Xe jet (o.d. 1 mm); (b) the monochromonator chamber, which is equipped with a gold-coated toroidal grating; (c) the beam source chamber, which houses a pulse valve (o.d. 0.7 mm) to produce a pulse molecular beam [the beam enters into the ionization chamber through a skimmer (o.d. 1 mm)]; (d) the ionization chamber, which houses an ion spectrometer and an electron time-of-flight (TOF) spectrometer together with a set of dual microchannel plate (MCP) detectors each for charge particle. A separate MCP detector is installed in this chamber to monitor the XUV intensity.

The electron signals from the pulsed field ionization and the XUV radiation were fed into two identical boxcars (SR 245, Stanford Research Systems) before further processing by a personal computer. The pulses used to synchronize the two pulse valves and the Nd:YAG laser were provided by a digital delay generator (DG 535, Stanford Research Systems). The pulse voltages for field ionization were provided by another DG 535 with a high voltage option.

The commercial samples, CH_3CN (purity 99.9%, from Tianjing chemical) and CD_3CN (99.9 atom % D, from Acros Organics), were used without further purification. The back pressures were the vapor pressures of the samples at room temperature. Care was taken to avoid the dimer and the auto-ionization signals' contamination of the real PFI-ZEKE signals.

III. Results and Discussion

Panels a and b of Figure 1 show the PFI-ZEKE spectra for CH_3CN and CD_3CN along with the assignments of the vibronic

TABLE 1: Vibronic Band Positions[a] and Assignments for the ZEKE Spectra of CH_3CN and CD_3CN

CH_3CN^+ ($\tilde{X}^2E$)		CD_3CN^+ ($\tilde{X}^2E$)	
observed	assignment[b,c]	observed	assignment[b,c]
235(5)	$(JT)^1$	196(5)	$(JT)^1$
		317(3)	$(JT)^2$
360(5)	$(JT)^3$		
554(3)	$(JT)^4$	487(3)	$(JT)^4$
683(3)	$(JT)^5$	603(3)	$(JT)^5$
		680(3)	$(JT)^7$
804(3)	4_0^1	825(3)	4_0^1
921(3)	$(JT)^9$		
1179(3)	6_0^1	943(3)	6_0^1
1620[d]	4_0^2		
2004(2)	2_0^1	2029(3)	2_0^1
2228(3)	$2_0^1(JT)^1$		
		2344[d]	$2_0^1(JT)^2$
2380(3)	$2_0^1(JT)^3$	2480(10)	$2_0^1(JT)^3$
2536(3)	$2_0^1(JT)^4$		
2661(5)	$2_0^1(JT)^5$		
2791(3)	$2_0^1 4_0^1$		
2908(5)	$2_0^1(JT)^9$		
3180(3)	$2_0^1 6_0^1$	2951(5)	$2_0^1 6_0^1$
3421(5)	$2_0^1 6_0^1(JT)^1$	3139(5)	$2_0^1 6_0^1(JT)^1$
3617[d]	$2_0^1 4_0^2$		
3982(3)	2_0^2	4004(5)	2_0^2

[a] The band positions are relative to the ionization potentials of CH_3CN and CD_3CN. The units are in cm^{-1}. The numbers in the parentheses are the uncertainties of the last digit. [b] Vibrational bands 2_0^n, 4_0^n, and 6_0^n represent the C≡N stretching (υ_2), the C−C stretching (υ_4), and the CH_3 (CD_3) deforming (υ_6) vibronic excitations from the ground state to the nth vibronic states, respectively. [c] $(JT)^n$ represents the Jahn−Teller active C−C≡N bending (υ_8) vibronic excitation. [d] With large uncertainty and the assignment is tentative.

bands of the corresponding ions. The pulsed electric fields used to ionize the samples were 0.85 V/cm. The resolutions of our instrument under these experimental conditions were about 2 cm^{-1}.[20,21] In Figure 1, there are blank regions where we could not obtain reliable ZEKE signals due to the very low efficiency of the four-wave mixing to produce the XUV light. The blank regions are from ~1280 to ~1430 cm^{-1} for CH_3CN and from ~1080 to ~1230 cm^{-1} for CD_3CN. The PFI-ZEKE signals have been normalized to the XUV intensities.

Because CH_3CN^+ ($\tilde{X}^2E$) (CD_3CN^+ ($\tilde{X}^2E$)) is formed by removing the electron in the C≡N bonding, the vibrational modes related to C−C≡N will be excited. From panels a and b of Figure 1, it is seen that the C−C≡N bending (υ_8), which is the Jahn−Teller active mode, the C≡N stretching (υ_2), the C−C stretching (υ_4), and the CH_3 (CD_3) deforming vibration (υ_6) modes are excited. Similar phenomena have been found in the high-resolution photoelectron spectroscopic and VUV photoabsorption studies.[8,10]

The spectra may be divided into two parts. The first part is the energy region from the IP to ~1100 cm^{-1}, where the C−C ≡ N bending excitations (υ_8) are the main excitation. In this paper, the Jahn−Teller active υ_8 mode is represented as $(JT)^n$, where n is the nth vibronic energy level of the υ_8 mode (see section III(a) for a detailed account). The second part is the energy region from ~1400 to ~4500 cm^{-1} above the IP where the vibronic bands of υ_8, υ_2, υ_4, and υ_6 are excited. The vibronic band positions and the assignments are listed in Table 1.

The first vibrational bands for CH_3CN^+ and CD_3CN^+ appear at 235 and 196 cm^{-1} in panels a and b of Figure 1, respectively. Because of the low resolutions of all the previous studies on CH_3CN^+ and CD_3CN^+, these two bands have not been observed.[1−8] These two frequencies are much lower than those of the neutrals, 362 cm^{-1} for CH_3CN and 331 cm^{-1} for CD_3CN.[17] The second lowest bands observed for CH_3CN^+ and CD_3CN^+ are 360 and 317 cm^{-1}, respectively. These are difficult to assign as the harmonics of the lowest vibrational bands observed. Even at first sight, the complicated vibrational structure may suggest that the Jahn−Teller coupling is operable here, as suggested by the previous studies.[4,8] In the following, we provide a detailed analysis of the vibronic structures shown in the first parts of panels a and b of Figure 1, employing a simple harmonic model that takes into account the linear and quadratic Jahn−Teller coupling terms.

(a) Jahn−Teller Coupling and Vibronic Band Assignments. The Jahn−Teller coupling will result in the splitting of degenerate vibrational energy levels or the forming of a vibronic structure. If we consider the Jahn−Teller coupling as a perturbation and only one degenerate mode is Jahn−Teller active, the perturbation matrix elements of the linear and quadratic coupling terms for a C_{3v} symmetry molecule ($\tilde{X}^2E$) can be written as the following,[11−13]

$$\langle \upsilon,\Lambda,\Sigma|H^{(0)}|\upsilon,\Lambda,\Sigma\rangle = (\upsilon+1)\omega_t + \xi\Lambda\Sigma \quad (1)$$

$$\langle -\Lambda;\upsilon',l-\Lambda,\Sigma|H_{JT}^{(1)}|\Lambda;\upsilon,l,\Sigma\rangle = \omega_t D_t^{1/2}\{[\upsilon-\Lambda l+2]^{1/2}\delta_{\upsilon',\upsilon+1} + [\upsilon+\Lambda l]^{1/2}\delta_{\upsilon',\upsilon-1}\} \quad (2)$$

$$\langle -\Lambda;\upsilon',l+2\Lambda,\Sigma|H_{JT}^{(2)}|\Lambda;\upsilon,l,\Sigma\rangle = \frac{1}{4}\omega_t K_t\{[(\upsilon+\Lambda l+4)(\upsilon+\Lambda l+2)]^{1/2}\delta_{\upsilon',\upsilon+2} + 2[(\upsilon+\Lambda l+2)(\upsilon-\Lambda l)]^{1/2}\delta_{\upsilon',\upsilon} + [(\upsilon-\Lambda l)(\upsilon-\Lambda l-2)]^{1/2}\delta_{\upsilon',\upsilon-2}\} \quad (3)$$

where $\Lambda(\pm1)$ and $\Sigma(\pm1/2)$ represent the quantum label for the projection of the electronic orbital angular momentum and the spin angular momentum on the C_{3v} symmetric axis, respectively. υ, l, and ξ represent the vibrational quantum number, the vibrational angular momentum, and the spin−orbit coupling constant, respectively. ω_t is the harmonic vibrational frequency for the Jahn−Teller active vibrational mode. D_t and K_t are the dimensionless linear and quadratic Jahn−Teller coupling constants, respectively, and they determine the splitting of the degenerate potential curve due to the Jahn−Teller coupling. Assuming the values of D_t, K_t, ω_t, and ξ, the vibronic energy levels can be calculated by solving the Hamitonian matrix equation with matrix elements shown in eqs 1−3.. Suitable truncations of the vibronic basis wave functions should be made to guarantee the convergence of the energy levels that are considered.

For CH_3CN^+ ($\tilde{X}^2E$) and CD_3CN^+ ($\tilde{X}^2E$), energy splittings due to the spin−orbit coupling may exist. The spin−orbit energy splitting for the first vibronic state of HCN^+ ($\tilde{X}^2\Pi$) has been determined to be 50 cm^{-1}.[22] Therefore, the spin−orbit energy splitting for CH_3CN^+ ($\tilde{X}^2E$) (CD_3CN^+ ($\tilde{X}^2E$)) is expected to be smaller than this number because of the quench of the orbital angular momentum due to the lowering of the symmetry. The first vibronic bands for CH_3CN^+ and CD_3CN^+ are shown in panels a and b of Figure 2, respectively. The pulse electric field strengths used to ionize the Rydberg molecules were 0.25 V/cm. In these conditions, our instrument has a resolution better than 1 cm^{-1}.[21] Even so, the first vibronic bands shown in Figure 2 do not show rotationally resolved structures and their bandwidths are around 40 cm^{-1}. The widths of some bands in panels a and b of Figure 1 are as narrow as 15 cm^{-1}, which are much narrower than the first vibronic bands. These phenomena

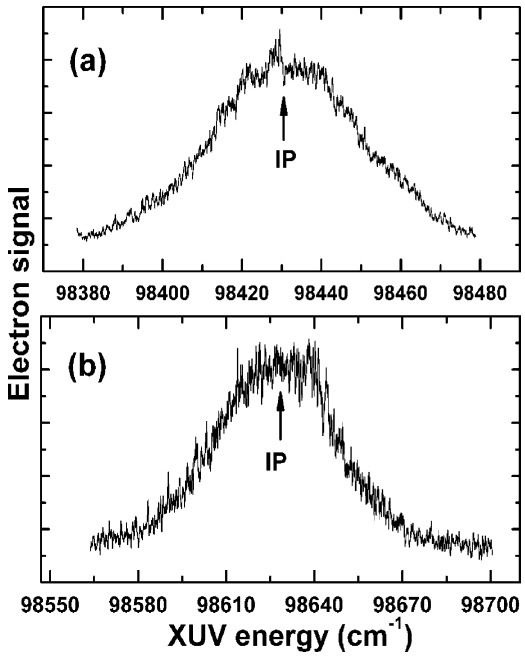

Figure 2. PFI-ZEKE spectra for the first vibronic bands of (a) CH_3CN and (b) CD_3CN. The pulse electric field strengths used to ionize the Rydberg molecules were 0.25 V/cm. After taking into account the Stark effect, the ionization potentials of CH_3CN and CD_3CN are determined as 98 432 ± 8 and 98 630 ± 8 cm^{-1}, respectively.

TABLE 2: Spectroscopic Constants[a] Used in the Fitting of the C−C≡N Bending Vibronic Energy Levels[b] (υ_8) for CH_3CN^+ ($\tilde{X}^2E$) and CD_3CN^+ ($\tilde{X}^2E$)

Molecule	ω_8	D_t	K_t
CH_3CN^+ ($\tilde{X}^2E$)	329	0.10	0.13
CD_3CN^+ ($\tilde{X}^2E$)	302	0.10	0.22

[a] The ω_8, D_t, and K_t represent the harmonic frequency for the C−C≡N bending vibration in cm^{-1}, the dimensionless linear, and the dimensionless quadratic Jahn−Teller coupling constants, respectively. [b] The comparisons of the calculated energy levels with those of the experimentally observed can be found in Figures 3 and 4.

indicate that the spin−orbit energy splittings may exist for the first vibronic bands. Unfortunately, we could not deconvolute the spectra to two spin−orbit components and, hence, determine the spin−orbit coupling constants. From the width of the first vibronic band, it is reasonable to guess that the spin−orbit splitting is around ~10 cm^{-1}. To fit the spectra, however, we simply assume that $\xi = 0$. The parameters used in the fitting are shown in Table 2. Figures 3 and 4 show the calculated energy levels and their symmetry assignments along with those observed. Because the Jahn−Teller effect mixes different vibrational states and the vibrational quantum numbers are not good quantum numbers anymore, we use the order of the energy levels to label the vibronic energy levels instead of the vibrational quantum numbers; that is, $(JT)^n$ means the nth energy level of the vibronic state. In Figures 3 and 4, we also list the leading terms of the basis functions, which contribute more than 10% to the wave functions of the corresponding energy levels.

Due to the coupling of the electronic motion with the degenerate vibration, the potential energy of the molecule will be shifted downward, and the shifted energy is called the Jahn−Teller stabilization energy. It can be calculated according to the formula[11−12]

$$\epsilon_{JT} = D_t\omega_t(1 + K_t) \quad (4)$$

Using the Jahn−Teller constants listed in Table 2, the stabilization energies for CH_3CN^+ ($\tilde{X}^2E$) and CD_3CN^+ ($\tilde{X}^2E$) are both calculated to be 37 cm^{-1}. This is in agreement with the requirement of the Born−Oppenheimer approximation that the stabilization energy should be only related to the electronic structure. There are only very small Jahn−Teller stabilization energies for CH_3CN^+ ($\tilde{X}^2E$) and CD_3CN^+ ($\tilde{X}^2E$); however, these small stabilization energies change the outlook of the ZEKE spectra drastically.

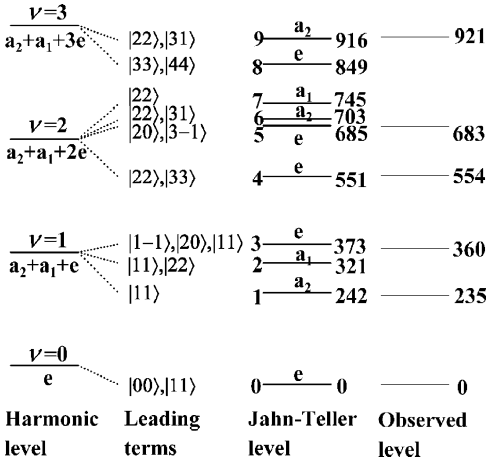

Figure 3. relative vibronic energy level diagram for the C−C≡N bending excitation (υ_8) in CH_3CN^+ ($\tilde{X}^2E$). In the figure, the *harmonic level* represents the calculated energy level using the simple harmonic model; the *Jahn−Teller level* represents the calculated energy level taking into account the linear and quadratic Jahn−Teller coupling terms (the coupling constants are listed in Table 2); the *observed level* is the energy level observed experimentally (see Table 1); the *leading terms* are the basis functions that contribute more than 10% to the wave functions of the corresponding energy levels. For the symbol $|xx\rangle$, the first number represents the vibrational quantum number υ and the second one represents the vibrational angular momentum quantum number l. For levels with a_1 and a_2 symmetries, only the basis functions with positive l are listed.

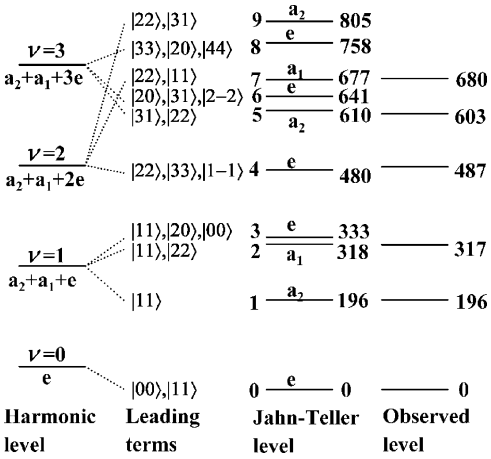

Figure 4. Relative vibronic energy level diagram for the C−C≡N bending excitation (υ_8) in CD_3CN^+ ($\tilde{X}^2E$). See the caption of Figure 3 for more details.

The vibrational band intensities of the ZEKE spectra may usually be described by the Franck−Condon (FC) factors.[20,23,24] Because of the Jahn−Teller effect in CH_3CN^+ ($\tilde{X}^2E$) and CD_3CN^+ ($\tilde{X}^2E$) and also the possible intensity borrowing of υ_8 by mixing with other symmetric vibrational modes, a good theoretical reproduction of the ZEKE spectra needs more than a simple FC calculation. This requires detailed theoretical studies in future.

(b) C≡N Stretching (υ_2), C−C Stretching (υ_4), and CH_3 (CD_3) Deforming (υ_6) Vibrations. Besides the Jahn−Teller

TABLE 3: First Adiabatic Ionization Potentials (IP) of CH_3CN and CD_3CN[a]

molecule	IP(eV)	uncertainty(eV)	method	reference[a]
CH_3CN	12.205	±0.004	PI[b]	2
	12.194	±0.005	PI[b]	4
	12.20	±0.01	PE[c]	7
	12.201	±0.02	PE[c]	8
	12.2040	±0.001	ZEKE[d]	this work
CD_3CN	12.23		PE[c]	5
	12.235	±0.005	PI[b]	4
	12.2286	±0.001	ZEKE[d]	this work

[a] A detailed list of IP by different experimental methods and authors can be found in ref 17. [b] By photoionization mass spectrometry. [c] By photoelectron spectroscopy. [d] By zero kinetic energy photoelectron spectroscopy. If there is spin−orbit energy splitting, the IP should be regarded as the average of the two spin-obit components.

active C−C≡N bending (υ_8) excitation, the C≡N stretching (υ_2), the C−C stretching (υ_4), and the CH_3 (CD_3) deforming (υ_6) vibrational excitations have also been observed, and their values and assignments are listed in Table 1. The fundamentals of the C≡N stretching and the C−C stretching vibrations have been observed in the previous PES spectra.[17] Our data with uncertainties around ±3 cm^{-1} (see Table 1) are within the large uncertainties of the previous data (±80 cm^{-1}). The CH_3 (CD_3) deforming vibration (υ_6) has not been reported previously. υ_6 is a degenerate vibration. Its observation also demonstrates the Jahn−Teller effect in CH_3CN^+ ($\tilde{X}^2E$) (CD_3CN^+ ($\tilde{X}^2E$)**)**. For the neutral, υ_6 is 1448 cm^{-1} for CH_3CN and 1046 cm^{-1} for CD_3CN.[17] Our data showed that the fundamentals of υ_6 are 1175 and 934 cm^{-1} for CH_3CN^+ ($\tilde{X}^2E$) and CD_3CN^+ ($\tilde{X}^2E$), respectively. For CH_3CN^+ ($\tilde{X}^2E$), the combination bands of the C≡N stretching (υ_2) with the Jahn−Teller active C−C≡N bending (υ_8) vibronic excitations are also highly excited. However, we could not obtain a good fit of the combination bands using eqs 1−3. The reason for this may be that the anharmonic terms in υ_8 or its coupling with other vibrational modes have not been considered in eqs 1−3. For CD_3CN^+ ($\tilde{X}^2E$), many fewer vibrational bands are found in the range of 1500−4500 cm^{-1}. The bands are also much broader than those in the first part of the spectra. The reason for this is not known to us. However, it is noted that that CD_3CN^+ has higher state densities than those of CH_3CN^+.

(c) Ionization Potentials (IP) of CH_3CN and CD_3CN. Panels a and b of Figure 2 show the first vibronic bands of the ZEKE spectra of CH_3CN and CD_3CN, respectively. To determine the IP, the band origin should be determined accurately and this can be done usually by simulation of the spectra.[20,21] In a simulation, the temperature of the molecular beam, the rotational constants for both the neutral and the ion, and the line strengths of the rotational transitions are needed. The rotational constants of CH_3CN have been determined as $A = 5.274$ cm^{-1} and $B = C = 0.307$ cm^{-1},[25] whereas the rotational constants of $CH_3CN^+(\tilde{X}^2E)$ have not been determined experimentally yet. As we stated in section III(a), the spin−orbit splitting may affect the widths of the spectra. Therefore, it is difficult to use a simple simulation here to determine the IP. However, the first vibrational bands are relatively symmetric, as shown in Figure 2. We simply used the band centers as the band origins. After taking into account the Stark effect, the ionization potentials are determined as 98 432 ± 8 cm^{-1} for CH_3CN and 98 630 ± 8 cm^{-1} for CD_3CN. Table 3 lists the previously reported values along with our results. The ionization potentials we measured, although with much higher accuracy than the previous data, are in agreement with the previous ones within their experimental uncertainties.

IV. Summary

The PFI-ZEKE spectra for CH_3CN and CD_3CN have been recorded in the regions from their ionization potentials to about 4500 cm^{-1} above them using coherent XUV radiation. The Jahn−Teller effect in CH_3CN^+ ($\tilde{X}^2E$) and CD_3CN^+ ($\tilde{X}^2E$) has been found experimentally. The spectra consist mainly of the Jahn−Teller active C−C≡N bending (υ_8), the C≡N stretching (υ_2), the CH_3 (CD_3) deforming (υ_6), and the C−C stretching (υ_4) vibronic excitations. The vibronic bands arising from the Jahn−Teller effect have been assigned with a harmonic model including linear and quadratic Jahn−Teller coupling terms, taking into account only the single mode (υ_8) vibronic excitation. The ionization potentials of CH_3CN and CD_3CN have been determined with a much higher accuracy than the previously reported data.

Acknowledgment. We are thankful to Professor C. Y. Ng for suggesting us to do this research. We also acknowledge the research supports by the National Science Foundation of China under Projects 20273038 and 10274041, the Specialized Research Fund for the Doctoral Program of Higher Education of China, and the NKBRSF of China.

References and Notes

(1) Watanabe, K.; Nakayama, T.; Mottl, J. *J. Quant. Spectrosc. Radiat. Transfer* **1962**, *2*, 369.
(2) Nicholson, A. J. C. *J. Chem. Phys.* **1965**, *43*, 1171.
(3) Dibeler, V. H.; Liston, K. S. *J. Chem. Phys.* **1968**, *48*, 4765.
(4) Rider, D. M.; Ray, G. W.; Darland, E. J.; Leroi, G. E. *J. Chem. Phys.* **1981**, *74*, 1652.
(5) Lake, R. F.; Thompson, H. *Proc. R. Soc. London* **1970,** *A317*, 187.
(6) Frost, D. C.; Herring, F. G.; McDowell, C. A.; Stenhouse, I. A. *Chem. Phys. Lett.* **1970**, *4*, 533.
(7) Staley, R. H.; Kleckner, J. E.; Beauchamp, J. L. *J. Am. Chem. Soc.* **1976**, *98*, 2081.
(8) Gochel-Dupuis, M.; Delwiche, J.; Hubin-Franskin, M. J.; Collin, J. E. *Chem. Phys. Lett.* **1992**, *193*, 41.
(9) Delwiche, J.; Gochel-Dupuis, M.; Collin, J. E.; Heinesch, J. *J. Electron Spectrosc. Relat. Phenom.* **1993**, *66*, 65.
(10) Eden, S.; Limao-Vieira, P.; Kendall, P.; Mason, N. J.; Hoffmann, S. V.; Spyrou, S. M. *Euro. Phys. J. D* **2003**, *26*, 201.
(11) Barckholtz, T. A.; Miller, T. A. *Int. Rev. Phys. Chem.* **1998**, *17*, 435.
(12) Applegate, B. E.; Barckholtz, T. A.; Miller, T. A. *Chem. Soc. Rev.* **2003**, *32*, 38.
(13) Hill, C.; Brown, J. M. *J. Mol. Spectrosc.* **2005**, *229*, 207.
(14) Choe, J. C. *Int. J. Mass Spectrom.* **2004**, *235*, 15.
(15) Hoper, U.; Botschwina, P.; Koppel, H. *J. Chem. Phys.* **2000**, *112*, 4132.
(16) Marenich, A. V.; Boggs, J. E. *J. Chem. Phys.* **2005**, *122*, 024308.
(17) Linstrom, P. J., Mallard, W. G.. Eds. *NIST Chemistry WebBook, NIST Standard Reference Database*; National Institute of Standards and Technology: Gaithersburg, MD, 20899; June 2005; Number 69 (http://webbook.nist.gov).
(18) Ng, C. Y. *Annu. Rev. Phys. Chem.* **2002**, *54*, 101 and references therein.
(19) Schlag, E. W. *ZEKE Spectroscopy;* Cambridge University Press: Cambridge, U.K., 1996.
(20) Mo, Y.; Yang, J.; Chen, C. *J. Chem. Phys.* **2004**, *120*, 1263.
(21) Yang, J.; Hao, Y.; Li, J.; Zhou, C.; Mo, Y. *J. Chem. Phys.* **2005**, *122*, 134308.
(22) Wiedmann, R. T.; White, M. G. *J. Chem. Phys.* **1995**, *102*, 5141.
(23) Yang, D. S.; Zgierski, M. Z.; Rayner, D. M.; Hackett, P. A.; Martinez, A.; Salahub, D. R.; Roy, P.-N.; Carrington, T., Jr. *J. Chem. Phys.* **1995**, *103*, 5335.
(24) Lee, M.; Kim, H.; Lee, Y. S.; Kim, M. S. *J. Chem. Phys.* **2005**, *123*, 024310.
(25) Simeckova, M.; Urban, S.; Fuchs, U.; Lewen, F.; Winnewisser, G.; Morino, I.; Yamada, K. M. T. *J. Mol. Spectrosc.* **2004**, *226*, 123.